Smart Charging of PEVs Penetrating into Residential Distribution Systems

Isha Sharma, *Student Member, IEEE,* Claudio Cañizares, *Fellow, IEEE,*
and Kankar Bhattacharya, *Senior Member, IEEE,*

***Abstract*—This paper presents a novel modeling framework for the analysis of Plug-in Electric Vehicle (PEV) charging in unbalanced, residential, distribution systems. A Smart Distribution Power Flow (SDPF) framework is proposed to determine the controlled or smart charging schedules and hence address the short-comings of uncontrolled charging. The effect of peak-demand constraint imposed by the Local Distribution Company (LDC) is also studied within the SDPF framework for the smart charging scenarios. Uncontrolled versus smart charging schemes are compared for various scenarios, from both the customer's and the LDC's perspective. Various objective functions, such as energy drawn by the LDC, total feeder losses, total cost of energy drawn by LDC and total cost of PEV charging are considered. Studies are carried out considering two sample systems i.e., the IEEE 13-node test feeder and a real distribution feeder. Analyses are also presented considering a probabilistic representation of the initial state of charge (SOC) and start time of charging for various scenarios to take into account the difference in customers' driving patterns. The results show that uncontrolled charging of PEVs results in increased peak demand, low node voltage levels, and increased feeder current magnitudes. On the other hand, the SDPF framework provides very satisfactory operating schedules for the overall system including smart PEV charging.**

***Index Terms*—Plug-in electric vehicles, Uncontrolled charging, smart charging, unbalanced distribution system, optimal feeder operation.**

I. Nomenclature

Indices

C	Controllable capacitor banks, $C \in n$.
C_n	Controllable capacitor banks at node n.
EV	PEV loads, $EV \in L$.
EV_n	PEV load at node n.
k	Hours, k = 1,2,...,24.
l	Series elements.
L	Loads, $L \in n$.
L_n	Loads at node n.
n	Nodes.
N_o	Set of nodes, $n \in N_o$.
p	Phases, $p = a, b, c$.
r	Receiving-end.
r_n	Receiving-ends connected at node n.
s	Sending-end.
s_n	Sending-ends connected at node n.
SS	Substation node, $SS \in n$.
t	Controllable tap changer, $t \in l$.

Parameters

ΔQ	Size of each capacitor block in capacitor banks [Var].
ΔS	Percentage voltage change for each LTC tap.
η	PEV charging efficiency.
γ	Average hourly load of a residence [W].
ρ	Hourly forecast market price [$/MWh].
τ	Time interval in hours [h].
θ	Load power factor angle [rad].
$ABCD$	Three-phase ABCD matrices; A unitless, B in Ω, C in Siemens, D unitless.
C^{max}	PEV battery capacity [Wh].
Ic^o	Load current at specified power and nominal voltage [A].
I^{max}	Maximum feeder current limits [A].
N	Number of PEVs owned by a residence.
$N^{'}$	Number of PEVs connected in each phase and node.
$\overline{N}$	Maximum number of capacitor blocks available in capacitor bank.
$\overline{P}$	Maximum power drawn by PEV battery [W].
PD	Load at n node [W].
Pc	Active power of load [W].
$\overline{PD}$	Maximum allowable peak demand [W].
Qc	Reactive power of load [Var].
SOC^f	Final state of charge of the PEV battery.
SOC^i	Initial state of charge of the PEV battery.
$\overline{tap}, \underline{tap}$	Maximum and minimum tap changer position.
V^o	Specified nominal voltage [V].
V^{max}	Maximum voltage limit [V].
V^{min}	Minimum voltage limit [V].
X	Reactance of capacitor [Ω].
Z	Load impedance at specified power and nominal voltage [Ω].

Variables

cap	Number of blocks of switched capacitor banks.
I	Current phasor [A].
$\overline{I}$	Vector of three-phase line current phasors [A].
I^o	Load current at nominal voltage [A].
$J_1 - J_4$	Objective functions.
P	Power drawn by PEV [W].
Q	Reactive power of capacitor banks [Var].
tap	Tap position.
V	Voltage phasor [V].
$\overline{V}$	Vector of three-phase line voltages [V].

This work is supported by the Natural Sciences and Engineering Research Council (NSERC) of Canada, Hydro One Inc., ABB US Corporate Research and IBM Canada.

The authors are with the Department of Electrical and Computer Engineering, University of Waterloo, Ontario, Canada N2L 3G1 (e-mail: {i4sharma, ccanizar, kankar}@uwaterloo.ca).

II. INTRODUCTION

PLUG-IN ELECTRIC VEHICLES (PEVs) will play a significant role in reducing greenhouse gas emissions from the transport sector and the sector's dependence on imported fossil fuels [1]. A PEV draws some, or all, of its power from the power grid. Recharging the PEV battery is typically carried out in residential garages equipped with standard outlets, and takes several hours. However, a specialized high voltage/high current electrical outlet can also be used for fast charging; using a higher level charging brings about significant reduction in charging time [2].

In Canada, the province of Ontario has an aggressive plan for the adoption of smart grid technologies in the distribution system, starting with the installation of smart meters. Time-of-use (TOU) tariffs have been introduced with the intention of reducing electricity use during peak hours. Technologies for convenient charging of PEVs are expected to be available by 2020 [1]. The Electric Vehicle Incentive Program provides incentives to customers from $5,000 - $8,500 (depending on battery capacity) towards the purchase or lease of a new PEV or battery electric vehicle [3]. It is estimated that the number of PEVs in the US and Canada would increase significantly by 2017-2018, resulting in considerable increase in charging demand [4], [5].

With increasing penetration of PEVs into distribution systems, there is a need to examine their effect on distribution feeders. In order to study the effect of PEV charging schedules on local distribution company's (LDC) system load profiles, a detailed analysis is needed considering PEV penetration levels and local concentrations.

The impact of coordinated charging, vis-$\grave{a}$-vis uncontrolled charging has been reported in various papers considering objective functions such as minimizing power losses and maximizing grid load factor [6], minimizing cost of charging and energy losses [7], and minimizing losses, and load factor maximization [8]. It is noted in these papers that uncoordinated charging leads to increased peak, decrease in distribution system efficiency and threatens grid performance and asset's life. These works are based on balanced distribution systems; thus, random placement of PEVs are studied, and balanced power flows are solved using traditional methods such as backward forward sweep ([6], [8]) or modified Newton-based load flow ([7]) to calculate node voltages and feeder currents.

A demand response strategy is proposed in [9] where customers can control their own loads based on their preferences and comfort levels; the PEV charging schedule is created based on a stochastic method for modeling driving patterns and home arrival times. A scheduling algorithm is proposed in [10] to determine the optimum power purchase schedule for an aggregate PEV fleet from a day-ahead electricity market. An algorithm is proposed to dispatch the purchased energy to PEV loads on the operating day. It is noted that there is a need to revise current market regulations for PEV loads to improve system reliability and operation. In [11], controlled charging of PEVs based on the charging behavior of a number of vehicles, users, travel data and LDC system data, is proposed. It is observed that the impact of PEV charging varies across areas and can be reduced by shifting some charging load to a commercial distribution system.

The effect of fast-charging PEVs in a distribution system is examined in [12] using power-flow, short-circuit and protection studies. It is observed that the location of charging station can limit the maximum number of vehicles being simultaneously charged within the operating limits. In [13], probabilistic power flow analysis is used to study the impact of uncontrolled PEV charging on the grid; a methodology is proposed to model PEV charging loads at a charging station and in a local residential community. PEV loads are modeled in [14] considering the stochastic nature of the start-time of battery charging and the initial State-of Charge (SOC).

This paper proposes a smart distribution system operation framework including PEV smart charging in LDC operations. The proposed framework is depicted in Fig. 1, where forecasted inputs of the LDC's load profile for the next day, real-time price (RTP), number of PEVs to be charged at a node and phase, and their initial SOC are available. Executing a Smart Distribution Power Flow (SDPF), which is based on a distribution optimal power flow model [15], the PEV smart charging schedules and operating decisions for taps, capacitors and switches for the next day can be determined. The SDPF model could be used within a Model Predictive Control (MPC) framework to revise its operating decisions when there is discrepancy between the actual inputs from their forecast values [16]. The MPC can incorporate forecast and newly updated information to arrive at an improved set of optimal decisions. Thus, at a given time k, the forecast inputs available over a given time horizon (e.g. 24 h) can be used to solve the SDPF to obtain decisions over this time horizon; if there is a change in any of the inputs, the SDPF model could be rerun to obtain improved revised decisions. Subsequently, the time horizon would move forward for the next optimization stage. However, the proposed framework cannot be implemented within the existing communication infrastructure now available in distribution feeders; more sophisticated two-way communication devices would be necessary for both LDCs and customers to realize this approach.

This paper builds upon the preliminary work reported in [17], with several additional model improvements and case studies that allow to draw more relevant and important conclusions. Thus, the main differences and contributions of this paper over and above previous works in the subject including [17], are as follows:

- The SDPF mathematical model proposed in this paper is a comprehensive representation of the LDC's operating criteria in Smart Grids, since it represents customer's perspective in the LDC's decision making.
- The presented model includes a peak-demand constraint imposed by the LDC as a control mechanism to define customers their PEV charging schedules in real-time.
- This paper presents a thorough examination of uncontrolled PEV charging and its impact on LDC operation, and determines smart charging schedules for various relevant scenarios.
- The proposed SDPF model is also tested on a realistic distribution feeder presented in [15].

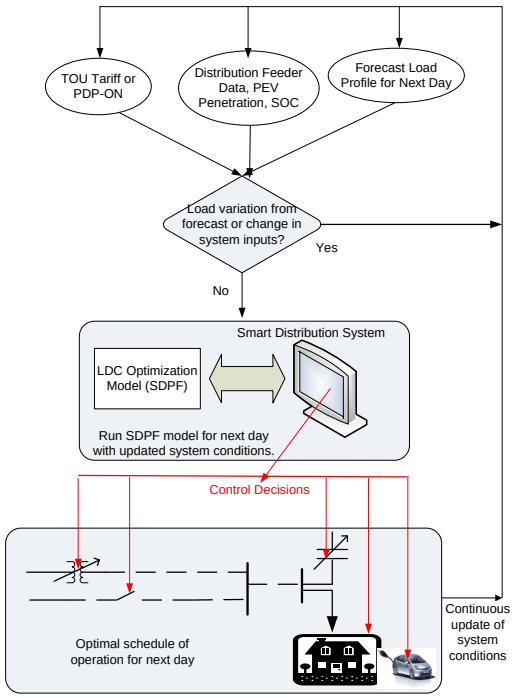

Fig. 1. Smart distribution system operation framework.

- Two different load models are considered, i.e., constant impedance and ZIP loads, for the analysis.
- A probabilistic representation of the initial SOC and starting time of charging is considered, to take into account different customers' driving patterns.

The rest of the paper is structured as follows: Section III presents the mathematical model of the proposed SDPF and discusses various objective functions, considered in this paper, from LDC's and customers' perspective. Section IV presents the main assumptions made in this work and description of the scenarios constructed for the analyses. Section V discusses the results obtained from various case studies and scenario analyses carried out using the IEEE 13-node test feeder and a real feeder. Section VI highlights the main conclusions from this research.

III. Operations Model of a Smart Distribution System

A. Three-phase Distribution System

A generic distribution system comprises series and shunt components. The series components include conductors / cables, transformers, transformer load tap changers (LTCs) and switches which are modeled using ABCD parameters, computed from relationships between sending and receiving end voltages and currents [18]:

$$\begin{bmatrix} \overline{V}_{s,p,k} \\ \overline{I}_{s,p,k} \end{bmatrix} = \begin{bmatrix} A_{(l\times p)} & B_{(l\times p)} \\ C_{(l\times p)} & D_{(l\times p)} \end{bmatrix} \begin{bmatrix} \overline{V}_{r,p,k} \\ \overline{I}_{r,p,k} \end{bmatrix} \quad \forall l, \forall p, \forall k \tag{1}$$

The ABCD parameters for conductors, cables, transformers and switches are constants. Switches are represented as zero impedances, conductors and cables as π-equivalent circuits, and three-phase transformers are modeled based on the type of connection (wye or delta). Voltage regulating transformers in a distribution system are equipped with LTCs, whose ABCD parameters cannot be considered constant since they depend on the tap position at a given time k. Thus, B and C are null matrices while the A and D matrices of the LTCs are modeled using the following equations:

$$A_{t,k} = \begin{bmatrix} 1+\Delta S\, tap_{t,a,k} & 0 & 0 \\ 0 & 1+\Delta S\, tap_{t,b,k} & 0 \\ 0 & 0 & 1+\Delta S\, tap_{t,c,k} \end{bmatrix} \tag{2}$$

$$D_{(t\times k)} = A^{-1}_{(t\times k)} \qquad \forall t, \forall p, \forall k \tag{3}$$

where $tap_{t,a,k}$, $tap_{t,b,k}$ and $tap_{t,c,k}$ are tap controls in the respective phases for the LTC and are considered continuous variables, which can take any value between -16 and +16, for a 32-step LTC. For a three-phase tap changer, the tap operations are considered identical in the three phases:

$$tap_{t,a,k} = tap_{t,b,k} = tap_{t,c,k} \qquad \forall t, \forall k \tag{4}$$

Shunt components comprise loads and capacitor banks and are modeled separately to represent unbalanced three-phase loads. In distribution systems, the electrical loads are typically modeled as voltage dependent to better represent the types of loads encountered in distribution feeders [19]. In this work, at first, the loads are modeled as constant impedance, with the following equations representing wye-connected impedance loads on a per-phase basis:

$$V_{L,p,k} = Z_{L,p,k} I_{L,p,k} \qquad \forall L, \forall p, \forall k \tag{5}$$

Subsequently, a mix of types of loads such as constant impedance (Z), constant current (I), and constant power (P), i.e, ZIP loads, are considered. Capacitor banks are modeled as multiple capacitor blocks with switching options, on a per-phase basis, as follows:

$$V_{C,p,k} = X_{C,p,k} I_{C,p,k} \qquad \forall C, \forall p, \forall k \tag{6}$$

$$jX_{C,p,k} = j\frac{V^{o2}_{C,p,k}}{Q_{C,p,k}} \qquad \forall C, \forall p, \forall k \tag{7}$$

$$Q_{C,p,k} = cap_{C,p,k}\ \Delta Q_{C,p,k} \qquad \forall C, \forall p, \forall k \tag{8}$$

where the variable, $cap_{C,p,k}$ is a continuous variable, and can take any positive value from 0 to $\overline{N}_{C,p}$. The PEV is modeled as a controlled current load, on a per-phase basis, as follows:

$$|I_{EV,p,k}|(\angle V_{EV,p,k} - \angle I_{EV,p,k}) = |I^{o}{}_{EV,p,k}|\angle\theta_{EV,p,k} \qquad \forall EV, \forall p, \forall k \tag{9}$$

$$Re(V_{EV,p,k} I^{*}_{EV,p,k}) = P_{EV,p,k} \qquad \forall k, \forall p, \forall EV \tag{10}$$

It is assumed that no significant reactive power is drawn by the PEV loads, thus treating them as unity power factor loads. Furthermore, the total energy drawn by the PEV battery over

the charging period, taking into account its efficiency η_{EV}, is equal to the battery charging capacity; thus:

$$\tau \sum_{k} \eta_{EV} P_{EV,p,k} = (SOC^{f}_{EV,p} - SOC^{i}_{EV,p}) C^{max}_{EV,p} N^{'}_{EV,p} \quad \forall EV, \forall p \quad (11)$$

The maximum power that can be drawn by the battery is constrained by $\overline{P}_{EV}$, the socket capacity of a standard electrical outlet, which depends on the level of charging, as follows:

$$P_{EV,p,k} \leq \overline{P}_{EV} N^{'}_{EV,p} \quad \forall EV, \forall p, \forall k \quad (12)$$

Equations (1)-(12) represent the various components of the three-phase distribution system including the PEV loads. To model the distribution system in its totality, these elements are required to satisfy the current balance at each node and phase:

$$\sum_{l} I_{l,p,k}(\forall r_n) = \sum_{l} I_{l,p,k}(\forall s_n) + \sum_{L} I_{L_n,p,k} + \sum_{C} I_{C_n,p,k} + \sum_{EV} I_{EV_n,p,k} \quad \forall n, \forall p, \forall k \quad (13)$$

And the voltage at the node and phase, at which a given set of components are connected, are the same as the corresponding nodal voltages:

$$V_{l,p,k}(\forall s_n) = V_{l,p,k}(\forall r_n) = V_{L_n,p,k} = V_{C_n,p,k} = V_{EV_n,p,k} \quad \forall p, \forall n, \forall k \quad (14)$$

B. Smart Distribution System Operation

The three-phase SDPF model determines the PEV charging schedules for various objective functions, considering the specified range of charging periods and grid operational constraints. The decision variables in the proposed SDPF model are the power drawn by the aggregate PEV loads at each node and phase, and the taps and capacitor switching decisions while the nodal voltages and feeder currents are the state variables. The different objective functions considered in this work represent the perspectives of the LDC and the customers, as follows:

- Minimize the total energy drawn by the LDC over a day, from the external grid:

$$J_1 = \sum_{k} \sum_{p} Re\left(V_{SS,p,k} I^{*}_{SS,p,k}\right) \quad (15)$$

  This objective (15) represents a situation where the LDCs are stipulated by regulatory agencies, as in Ontario, Canada, to bring about a reduction in their energy consumption levels.
- Minimize total feeder losses over a day:

$$J_2 = \sum_{k} \sum_{p} \sum_{n} Re\left(V_{s_n,p,k} I^{*}_{s_n,p,k} - V_{r_n,p,k} I^{*}_{r_n,p,k}\right) \quad (16)$$

  In the analysis of distribution systems, where loads are modeled to be voltage dependent, this objective seeks to improve the voltage profile across distribution nodes.
- Minimize the total cost of energy drawn by the LDC from the external grid, over a day:

$$J_3 = \sum_{k} \left(\sum_{p} Re(V_{SS,p,k} I^{*}_{SS,p,k}) \right) \rho(k) \quad (17)$$

  Here, $\rho(k)$ is the hourly price at which the LDC procures its energy from the external system. This price is generic and need not depend on the market structure. Thus, it can be the day-ahead price if there exits a day-ahead market settlement process, or the day-ahead forecast of the real-time price, or even a fixed price or tariff.
- Minimize the total cost of PEV charging:

$$J_4 = \sum_{k} \left(\sum_{p} \sum_{EV} P_{EV,p,k} \right) \rho_1(k) \quad (18)$$

  This objective can be used by the LDC to study the system impact of PEV charging, expecting rational behavior of customers, i.e. customers seeking to minimize their charging costs. It is assumed that all customer homes are equipped with smart meters and are subject to RTP or TOU tariffs $\rho_1(k)$, about which the customers are assumed to have sufficient information, so that they schedule their PEV charging accordingly. In real life, the two prices $\rho(k)$ and $\rho_1(k)$, are different from each other, because of the LDC's network costs, global adjustments, etc., included in the latter. However, in this paper, it is assumed that $\rho(k)$ is equal to $\rho_1(k)$ without loss of generality. In such a situation, the LDC needs to understand the system impact of such a charging approach, which is carried out using J_4.

The 3-phase distribution feeder and its components, modeled by (1)-(12), and the network equations (13)-(14), are the constraints of the SDPF model. Other constraints of SDPF model comprise the feeder operating limits that include the limits on node voltages, feeder currents, taps, and capacitors, as follows:

$$V^{min} \leq |V_{n,p,k}| \leq V^{max} \quad \forall n, \forall p, \forall k \quad (19)$$

$$|I_{i,j,p,k}| \leq I^{max}_{i,j} \quad \forall i \in s_n, \forall j \in r_n, \forall p, \forall k \quad (20)$$

$$\underline{tap}_{t,p} \leq tap_{t,p,k} \leq \overline{tap}_{t,p} \quad \forall t, \forall p, \forall k \quad (21)$$

$$0 \leq cap_{C,p,k} \leq \overline{N}_{C,p} \quad \forall C, \forall p, \forall k \quad (22)$$

The LDC may also impose a peak demand constraint, based on its substation capacity, as follows:

$$\sum_{L_n} \sum_{p} \left\{ Re\left(V_{L_n,p,k} I^{*}_{L_n,p,k}\right) + P_{EV,p,k} \right\} \leq \overline{PD}_k \quad (23)$$

The proposed SDPF model given by (1)-(23) is a non-linear programming (NLP) problem, which is modeled in GAMS and solved using the SNOPT solver [20]. In this paper, the taps and capacitors are modeled as continuous variables, as mentioned earlier, to alleviate the introduction of integer variables and hence retain the model as an NLP problem, thereby keeping the computational burden reasonable, considering that the main purpose of the paper is to study the impact of PEV

charging on feeders, and not the optimal voltage control of these feeders.

The output of the SDPF pertaining to the PEVs is the aggregated power drawn by PEV loads, at an hour, node and phase ($P_{EV,p,k}$). The PEV charging current ($I^o_{EV,p,k}$) can then be obtained from the model. In order to determine the number of PEVs to be charged, $P_{EV,p,k}$ can be used, after the optimization solution is obtained, as follows:

$$N^{chg}_{EV,p,k} = \frac{P_{EV,p,k}}{\overline{P}_{EV}} \tag{24}$$

For example, from the above equation, if a $P_{EV,p,k}$ = 17 kW is obtained, and knowing that $\overline{P}_{EV}$ = 4.8 kW, using (24), $N^{chg}_{EV,p,k}$ is calculated to be 3.54. From this, the LDC can infer that there should be three PEVs allowed to charge at this node, phase and hour, drawing 4.8 kW each, while a fourth PEV should be allowed to only draw 2.6 kW. Note that the determination of individual PEV charging levels is not considered here, since the objective is to study the charging problem from the feeder perspective; in this context, the simple method outlined above is one reasonable way to determine the number of PEVs charging at a node and phase.

IV. Assumptions and Scenarios

A. Assumptions

In order to evaluate the system impact of smart charging of PEVs vis-à-vis their uncontrolled charging, the following assumptions are made:

- A 24 h time horizon is assumed, with time interval of τ=1h. However, the proposed SDPF can accomodate smaller time steps if required, but at the cost of increased computational costs.
- Mid-size sedans, PHEV30 km with 9.76 kWh [21] battery capacities are considered. PHEV30 km implies that 60% of the vehicle kilometers are driven on battery and the rest on gasoline [22].
- PEVs are the only dispatchable loads at a node and are not capable of delivering power back to the grid. Note that it has been assumed that all the PEVs at a node and phase are aggregated, which is reasonable in the context of the studies presented here that concentrate on the feeder.
- Since all PEVs are assumed to be residential loads, these are not available for charging between 7 AM to 5 PM, when people are at work.
- The charging efficiency η_{EV} is assumed to be 85%, and only Level 2 charging (208-240V/40-100A) is considered.
- For the deterministic studies, the SOC of the PEV battery at the start of charging is 20% and it is charged to 90% of its full capacity at every node. In probabilistic studies, lognormal distribution of initial SOC is considered for each node.
- In deterministic studies, all the PEVs are assumed to have a minimum charging time of 2 hours [23], since the value of $\overline{P}_{EV}$ considered is 4.8 kW [1]. For probabilistic studies, the minimum charging time of PEVs depends on the initial SOC.
- The charging current of the PEV is assumed to remain constant and not vary with the SOC of the battery.

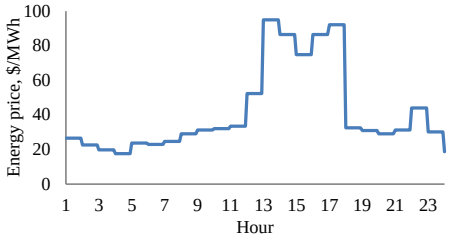

Fig. 2. Ontario HOEP for a weekday on 30 June, 2011.

- The entire load at a node on the feeder section, denoted by $PD_{p,L}$, are residential loads. Furthermore, it is assumed that if a house owns a PEV, it owns exactly $N_{p,L} = 1$ number of vehicles.
- The average monthly electricity consumption of a residence is 1500 kWh [24]. The average hourly load of the residence (γ) is calculated to be 2.08 kW.
- As mentioned in Section III.B, $\rho(k)$ is assumed equal to $\rho_1(k)$. In this paper, these prices are assumed to be the Hourly Ontario Electricity Price (HOEP) which applies to participants in the wholesale electricity market of Ontario ([25], [26]) and is used for all the analysis reported here. This HOEP is an hourly price, uniform across all of Ontario, computed at the end of every hour of real-time operation of the Ontario electricity market. The HOEP profile used is depicted in Fig. 2, wherein it can be noted that peak prices occur from hours 13-18.

Using the aforementioned assumptions, the number of PEVs connected in each phase and node, $N^{'}_{n,p}$, can be realistically estimated for an x p.u. penetration of PEV by:

$$N^{'}_{n,p} = floor\left(x\ floor\left(\frac{PD_{n,p}}{\gamma}\right)N_{p,L}\right) \quad \forall n, \forall p \tag{25}$$

A penetration of x = 1.0 means that every residence has one PEV, while x = 0 is the base case with no PEVs in the system. All analysis presented in this paper are carried out for x = 0.5 (*i.e., a PEV penetration of 50%, which means every second house has a PEV*), the PEV load being added to the existing distribution system, spread over the 13-hour charging period.

B. Scenarios

1) Business as Usual: Uncontrolled Charging (Case 1): This case assumes that customers charge their PEVs as and when they want to, without any regard for system constraints. The LDC has no control on the PEV charging schedules and hence an uncontrolled mode charging takes place. The following two scenarios are considered in this case, as presented in Table I.

S_1: This scenario assumes that the customers charge their PEVs in the shortest possible time (two hours), after plugging in. Although, they are not interested in minimizing the charging cost, they are aware of the prevailing tariff rates, for example, that the off-peak TOU price begins at 7 PM, as in Ontario [27], or that the off-peak RTP commences from 7 PM as shown in Fig. 2. Accordingly, PEV charging is carried out between 8 to 10 PM. Also since node voltages or feeder

TABLE I
SCENARIOS OF UNCONTROLLED CHARGING

	S_1	S_2
Objective Function	None	J_4
Nodal voltage limits	No	No
Feeder current limits	No	No
System peak demand constraint	No	No
Charging period	20, 21 h	1-6, 18-24 h

TABLE II
SCENARIOS OF SMART CHARGING

	S_3	S_4	S_5	S_6
Objective Function	J_1	J_2	J_3	J_4
Nodal voltage limits	Yes			
Feeder current limits	Yes			
System peak demand constraint	Yes			
Charging period	1-6, 18-24 h			

current limits are not of concern, this scenario is simulated using a distribution load flow without any limits on node voltages or feeder currents. This scenario effectively represents the worst case, as it results in concentrated buildup of charging loads, which coincides with the period of peak demand on the distribution feeder.

S_2: This scenario assumes that customers receive fairly precise forecast of $\rho_1(k)$. And they are equipped with smart home energy management systems (e.g. [28]) that determines optimal operational schedules for various home appliances such as air conditioner or heating, washer, dryer, and other appliances, as well as PEV charging, so as to reduce their overall electricity cost. In this scenario, the LDC has no control on the PEV charging schedules, and hence limits on node voltages or feeder currents are not considered.

2) Smart Charging (Case 2): In smart charging, the LDC is envisaged to send control signals to PEVs for charging purpose, considering grid constraints such as node voltage limits and feeder current limits. The LDC may also impose the system peak-demand constraint (23) while determining the PEV charging schedules. The following four different smart charging scenarios are considered, as summarized in Table II:

S_3: In this scenario, the LDC minimizes the total energy drawn from the substation over a day, as per (15).

S_4: In this scenario, the LDC seeks to minimize the total feeder losses in the system over a day, as per (16).

S_5: In this scenario, the LDC minimizes the total cost of energy drawn from the external grid over a day, as per (17).

S_6: In this scenario, the LDC determines the charging schedules assuming rational behavior of customers, while at the same time respecting system constraints to prevent feeder problems. Node voltage limits and feeder current limits are considered while the LDC seeks to minimize the total cost of PEV charging over a day, as per (18). It should be noted that this scenario is the "controlled" or "smart" version of Scenario S_2.

V. RESULTS AND ANALYSIS

A. IEEE 13-Node Test Feeder

The IEEE 13-node test feeder (Fig. 3) [29] is used in this work to examine the proposed SDPF model and smart charging

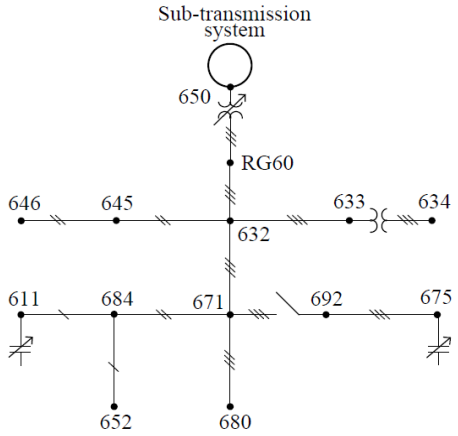

Fig. 3. IEEE 13-node test feeder [29].

TABLE III
NUMBER OF PEVS IN EACH NODE AND PHASE IN THE IEEE 13-NODE TEST FEEDER

Node	a	b	c
671	92	92	92
632-671	4	15	28
692	-	-	40
611	-	-	40
634	38	28	28
675	116	16	69
652	30	-	-
646	-	55	-
645	-	40	-

aspects of PEVs in distribution systems. As mentioned earlier, the capacitors are modeled as multiple capacitor banks with switching options; i.e., the capacitor at Bus 675 is assumed to comprise five capacitor blocks of 100 kVar in each phase, and that at Bus 611 comprising 5 capacitor blocks of 50 kVar in phase c. A 24-hour load profile is used in this work [17], for the analytical studies. The number of PEVs at each node and phase for a 50% penetration is given in Table III.

1) Case 1: Uncontrolled Charging

Figure 4 shows a comparison of the total system demand over a 24-hour period for the uncontrolled charging scenarios S_1 and S_2. Note that for S_1, a new peak is created at 9 PM and the system demand increases by 100% and 103% at 8 PM and 9 PM, respectively. On the other hand, in S_2 the charging occurs at 4 AM and at midnight, when the energy price is low, also creating new peaks in the system. Figure 5 shows how the main feeder (650-632) current is impacted in scenarios S_1 and S_2. Observe that the main feeder current exceeds the maximum limit in all three phases, thereby leading to possible feeder problems. Figure 6 shows that the node voltages drop significantly at 8 PM, especially in phases a and c, because of uncontrolled charging in S_1.

A summary comparison of the two scenarios of uncontrolled charging S_1 and S_2 is presented in Table IV. Note that for uncontrolled charging of PEVs without regard to charging costs or system conditions (S_1), the system impact is much more severe than when the PEV owners seek to minimize their charging costs (S_2). For instance, the energy drawn is

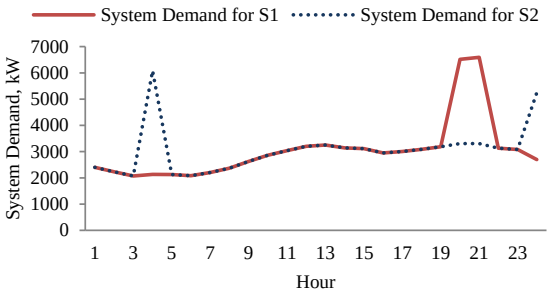

Fig. 4. Total demand for S_1 and S_2.

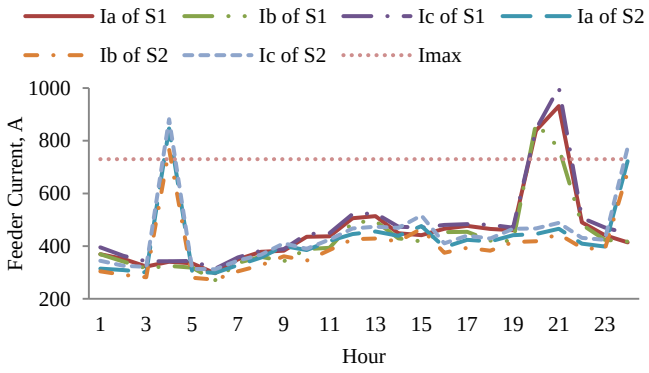

Fig. 5. Phase-wise Feeder 650-632 current for uncontrolled charging, S_1 and S_2.

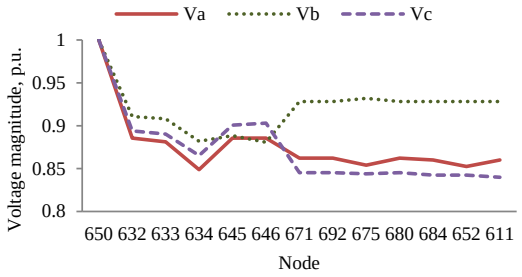

Fig. 6. Phase voltage magnitude at 8 PM in uncontrolled charging, S_1.

TABLE IV
SUMMARY RESULTS OF UNCONTROLLED PEV CHARGING SCENARIOS; 13-NODE FEEDER

	S_1	S_2	S_2 vs S_1 change [%]
Energy drawn by LDC [kWh]	73,727	68,669	-6.8
Feeder losses [kWh]	2,232	1,950	-12.6
PEV charging cost of customers [$/day]	196	117	-40.3
Cost of energy drawn by LDC [$/day]	3,119	2,806	-10

reduced by 6.8% and the PEV charging cost is reduced by 40.3% in S_2 as compared to S_1. However, as noted in Figs. 5 and 6, both S_1 and S_2 are detrimental to the system because feeder current limits are exceeded and several bus voltages are below acceptable limits.

2) Case 2: Smart Charging

a) Minimize Total Energy Drawn by LDC (S_3): Since the loads are modeled as voltage dependent, by operating

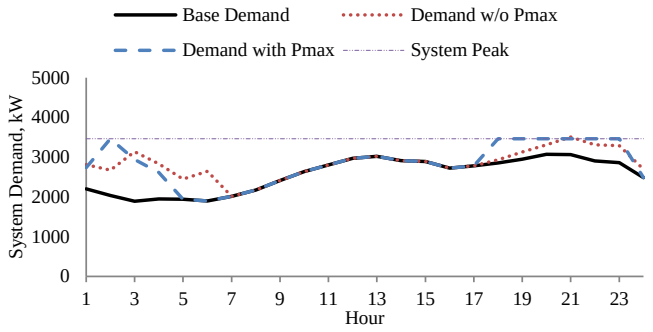

Fig. 7. Total demand with and without peak-demand constraint for S_3.

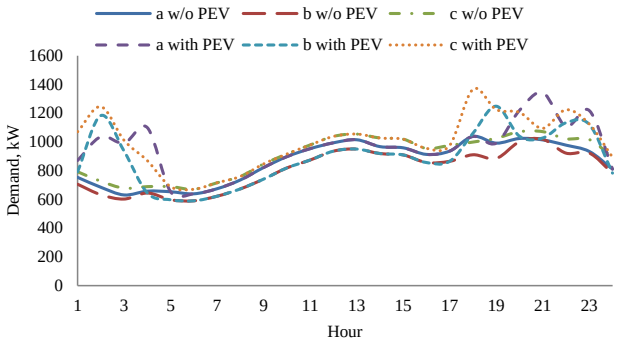

Fig. 8. Phase-wise total demand with and without PEV loads for S_3.

the system close to the lower acceptable voltage limit, (0.95 p.u.), the total energy drawn is minimized. Figure 7 shows the system base demand (without PEV loads) and the system demand profile including PEV charging loads, with and without the peak-demand constraint (23). The system demand exceeds $\overline{PD}$ at hour 21 because the PEV charging load coincides with the system peak at this hour. Note that when peak demand is limited, the PEV charging schedule is adjusted appropriately within the allowable charging hours, and the system demand is restricted. The base demands corresponding to scenarios S_3-S_5 are obtained by minimizing the respective objective function without considering PEVs, and the base demand in S_6 is obtained by subtracting the PEV charging load from the corresponding total demand.

Figure 8 presents the phase-wise demand with and without PEVs. Observe that the PEV charging mainly occurs during late evening and early morning hours. It should be mentioned that the feeder current magnitudes in this scenario are within limits, and the node voltages are observed to be close to 0.95 p.u.

b) Minimize Total Feeder Losses (S_4): Figure 9 shows that the resulting system demand including PEV charging load is below $\overline{PD}$, and thus constraint (23) is not imposed in this scenario. The nodal voltages improve and feeder current magnitudes are below their respective maximum limits. Furthermore, most of the PEV charging occurs in all phases during early morning hours, from midnight to 6 AM, when the base load is low, as shown in Fig. 10. This scenario results in a fairly flat load profile, without any steep peaks at any hour, as compared to other scenarios, and the node voltages

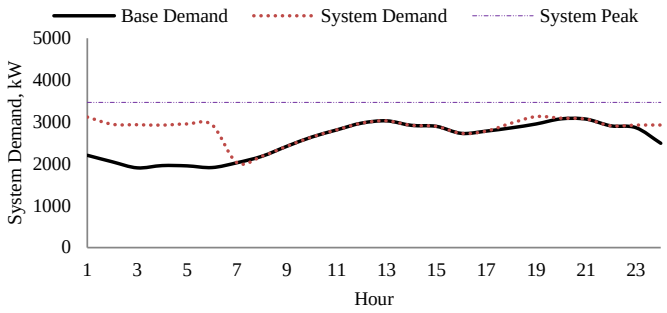

Fig. 9. Total demand for scenario S_4.

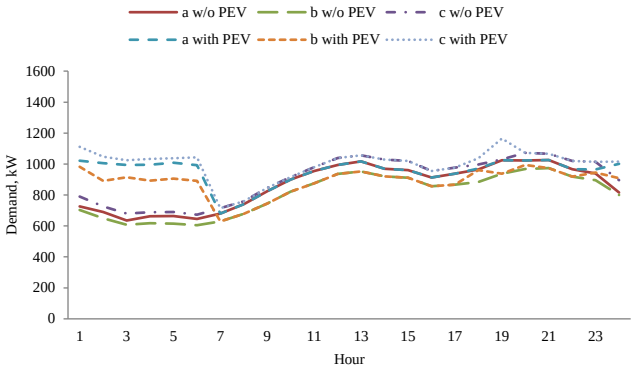

Fig. 10. Phase-wise total demand with and without PEV loads for S_4.

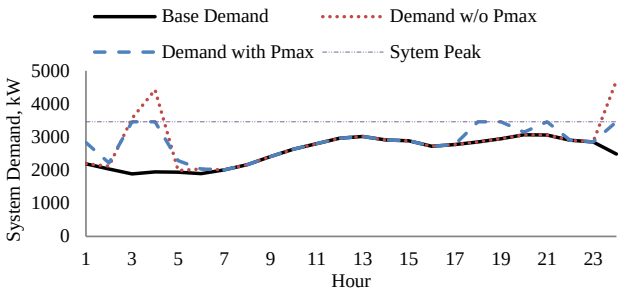

Fig. 11. Total demand with and without peak-demand constraint for S_5.

are significantly improved as compared to Scenario S_3.

c) Minimize Total Cost of Energy Drawn by LDC (S_5): Figure 11 shows the total system demand with and without peak-demand constraint (23), considering the PEV charging load. In this scenario, the LDC schedules the charging of PEV loads when electricity prices are low, i.e., at 4 AM, midnight and 3 AM. At midnight, the PEV charging load added to the system base load results in a system peak.

Because of the increase in demand when electricity prices are low, some feeder current magnitudes reach their maximum limit at midnight and 4 AM. By including constraint (23) in SDPF, the feeder current magnitudes are reduced below their maximum limit. Consequently, the PEV charging load is now distributed across more hours, as shown in Fig. 12. Voltages obtained in this scenario are close to their lower limit (0.95 p.u.), resulting in less energy drawn from the external grid.

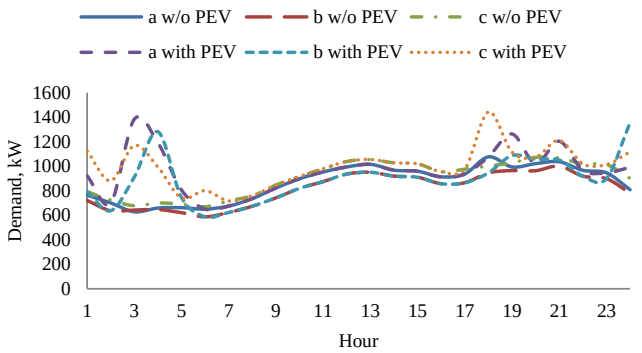

Fig. 12. Phase-wise total demand with and without PEV loads for S_5.

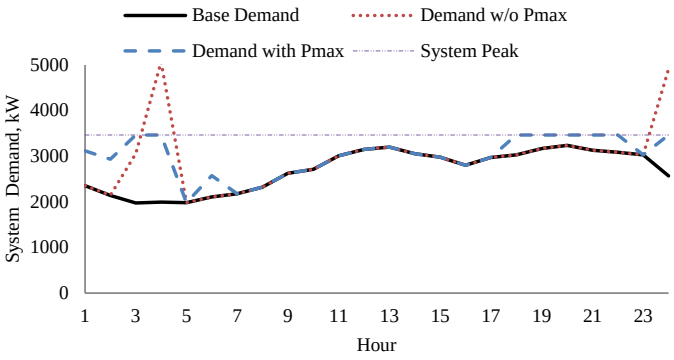

Fig. 13. Total demand with and without peak-demand constraint for S_6.

d) Minimize Total Cost of PEV Charging (S_6): In this scenario, the LDC schedules the charging of PEV loads considering the system limits, and at the same time assumes that customers behave rationally and seek to minimize their charging cost. From Fig. 13, it is seen that when the peak-demand constraint (23) is not imposed, the PEV charging is concentrated at 4 AM and midnight when electricity prices are low. This results in a significant increase in system demand at these hours. On the other hand, by imposing constraint (23), the PEV charging load is distributed over the next available cheap price hours. The phase-wise PEV charging schedules are shown in Fig. 14.

Since the PEV charging load is concentrated at 4 AM and at midnight, some feeder current magnitudes reach their maximum limits. Imposition of constraint (23) does not reduce these feeder currents below their limits, since the system is operating at the limits, which is undesirable. Since minimization of energy drawn is not an objective for this scenario, the voltages are observed to be above their lower limits.

B. Comparison of Smart Charging Scenarios

A comparison of the total energy drawn by the LDC, total feeder losses, total cost of energy drawn by the LDC and the total PEV charging cost, for scenarios S_3, S_4, S_5 and S_6 are presented in Table V. As expected, minimum energy drawn by the LDC from the external grid is obtained in S_3, although the PEV charging cost for customers is maximum, because of the way their charging is scheduled by the LDC. On the other hand, S_6 results in the lowest PEV charging cost for the

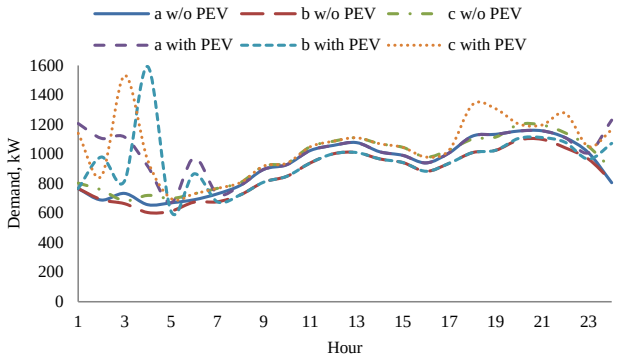

Fig. 14. Phase-wise total demand with and without PEV loads for S_6.

TABLE V
SUMMARY RESULTS OF SMART PEV CHARGING SCENARIOS; 13-NODE FEEDER

	S_3	S_4	S_5	S_6
Energy drawn by LDC [kWh]	69,593	69,715	69,738	73,127
Feeder losses [kWh]	1,829	1,790	1,870	2,035
PEV charging cost of customers [$/day]	162	146	122	119
Cost of energy drawn by LDC [$/day]	2,897	2,886	2,860	3,005

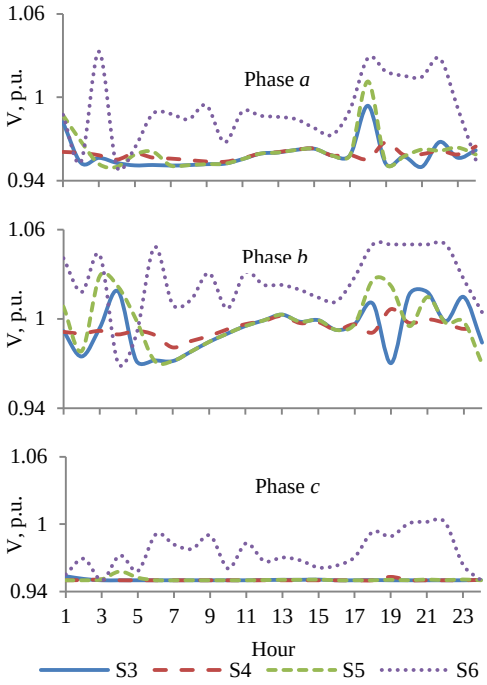

Fig. 15. Phase-wise voltages at Node 675 for S_3-S_6.

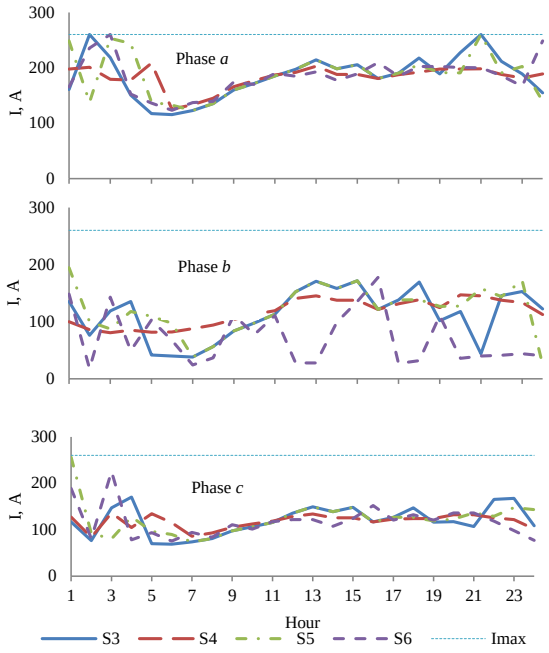

Fig. 16. Phase-wise Feeder 692-675 current for S_3-S_6.

customers, but requires the LDC to draw significantly larger amount of energy from the grid, thereby increasing cost and losses for the LDC.

An interesting observation can be made for scenario S_5, which seems to be the optimal choice for both the LDC and the customer from their respective perspectives. This scenario results in almost close to minimum PEV charging cost for the customers, while at the same time ensures that the LDC's energy drawn, feeder losses and cost of energy drawn are within acceptable values. Observe that scenario S_4 also yields reasonably balanced results for both the customers and the LDC.

Figure 15 shows the phase-wise voltage magnitudes for the various smart charging scenarios. Scenario S_3 shows voltages close to 0.95 p.u., which results in reduction of energy drawn by the LDC. Since phase c is the most heavily loaded as compared to other phases, voltages in this phase are close to 0.95 p.u. for S_3-S_5. On the other hand, scenario S_6 results in somewhat higher voltages, closer to 1 p.u., in all phases, as compared to the other scenarios, since neither the system energy demand nor feeder losses are minimized in this case.

Figure 16 presents phase-wise currents of Feeder 692-675 for all smart charging scenarios. Observe that the feeder current in phase a for S_3, S_5 and S_6 are at its maximum limit for some hours, while phases b and c (mostly) are below the maximum limit.

C. Effect of ZIP Load Models on PEV Smart Charging

The analysis presented in this paper thus far, considered only constant impedance loads. However, in order to examine the charging impact for a broader-based representation of loads, a mix of constant impedance (Z), constant current (I), and constant power (P) loads, i.e., ZIP loads, are also considered, to account for other possible types of loads. While constant impedance loads are modeled using (5), constant power loads are modeled as follows:

$$Pc_{L,p,k} + jQc_{L,p,k} = V_{L,p,k} I^*_{L,p,k} \qquad \forall L, \forall p, \forall k \quad (26)$$

and constant current loads are modeled as:

$$|I_{L,p,k}|(\angle V_{L,p,k} - \angle I_{L,p,k}) = |Ic^o{}_{L,p,k}|\angle\theta_{L,p,k}$$

$$\forall L, \forall p, \forall k \qquad (27)$$

Thus, in the proposed SDPF model, (26) and (27) are included along with other equations. To model voltage independent loads, and thus analyze the opposite case to the previous studies, the ZIP load mix is assumed to be dominated by constant power loads. Hence, loads at nodes 634, 645, 671, 675, and 632-671 are modeled as constant power loads; loads at nodes 646 and 652 are modeled as constant impedance loads; and finally loads at nodes 692 and 611 are modeled as constant current loads.

From the smart charging scenario studies it is noted that there is no significant change in the PEV charging schedules when compared to those with constant impedance loads. Accordingly, observe that there is very little effect of the load models on PEV charging cost. Table VI presents the summary results of the smart charging scenarios considering ZIP loads. All the scenarios depict an increase in energy drawn from the substation, feeder losses, and cost of energy drawn from the substation as compared to scenarios with constant impedance loads (Table V). As expected, since the ZIP loads are dominated by constant power, hence their energy consumption does not depend on the node voltages.

Figure 17 presents the phase voltage magnitudes at Node 675 for the smart charging scenarios with ZIP loads. Comparing these with those obtained with constant impedance loads (Fig. 15), it is noted that the voltage profiles are very similar for scenarios S_3, S_5 and S_6. In scenario S_4, the voltage profiles at Node 675 is significantly improved with ZIP loads. However, it is very difficult to draw general conclusions on the impact of loads models on node voltages by analyzing individual nodes. Therefore, an aggregated, phase-wise, voltage deviation index (VDI) is defined, as follows:

$$VDI_p = \sum_k \sum_n \left[V_{n,p,k} - V^{min}\right] \qquad (28)$$

Thus, in the 13-node test feeder considered, when all the node voltages are at V^{min} in a given phase p, the value of VDI will be zero, while when all node voltages are equal to 1 p.u., the VDI will take a value of 14.4. This implies that a low value of VDI indicate node voltages close to V^{min}, while VDIs close to or higher than 14.4 indicate a node voltage profile close to or above 1.0 p.u. Table VII presents phase-wise VDIs for constant impedance and ZIP load models, from which the following observations can be made:

- Constant impedance loads have low VDIs, in general, as compared to ZIP loads, implying that ZIP loads result in better voltage profiles.
- In all the scenarios, with both load models, the values of VDI_c are the lowest, since phase c is the most heavily loaded amongst the three phases.
- S_6 presents good voltage profiles, as evident from the high values of VDIs with both load models.
- S_4 with ZIP load models shows improved voltage profiles as compared to constant impedance loads.

Even though constant power loads are pre-dominant in the ZIP load models used, about 11% of the loads in phase a, 22% in phase b, and 27% in phase c are either constant impedance or constant current loads. This makes the behavior of the feeder different from a feeder with constant power loads only. Therefore, in S_3, voltages are close to their minimum allowable limits to draw minimum energy, while in S_4, voltages tend to improve so as to minimize the feeder losses, as shown in Table VII.

TABLE VI
SUMMARY RESULTS OF SMART CHARGING SCENARIOS WITH ZIP LOADS

	S_3	S_4	S_5	S_6
Energy drawn by LDC [kWh]	74,132	75,299	74,302	74,945
Feeder losses [kWh]	2,071	1,905	2,106	2,091
PEV charging cost of customers [$/day]	146	146	120	119
Cost of energy drawn by LDC [$/day]	3,077	3,118	3,054	3,076

TABLE VII
VDI FOR SMART CHARGING SCENARIOS WITH ZIP AND CONSTANT IMPEDANCE LOADS

	Constant Z Loads			ZIP Loads		
	a	*b*	*c*	*a*	*b*	*c*
S_3	5.52	9.60	3.97	7.02	12.42	4.01
S_4	5.50	9.61	3.90	19.54	24.17	17.04
S_5	6.09	10.41	4.10	7.23	12.58	4.19
S_6	14.59	18.93	11.73	15.57	20.40	11.83

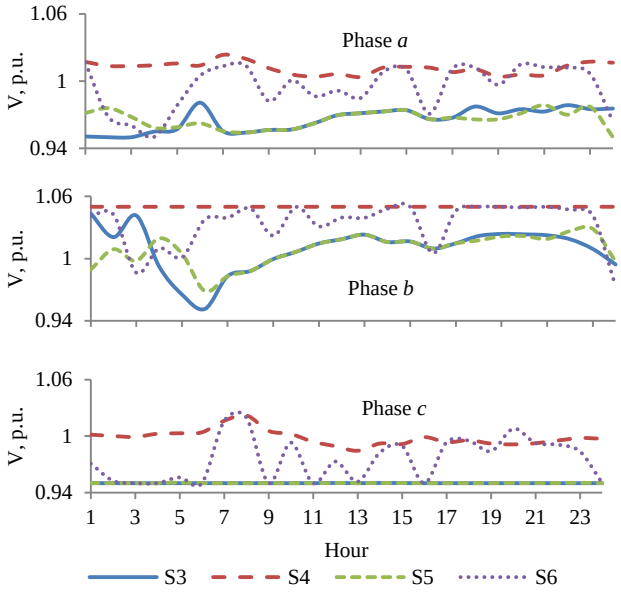

Fig. 17. Phase-wise voltages at Node 675 for ZIP loads, S_3-S_6.

D. Probabilistic Analysis

1) Uncontrolled Charging Scenario (S_1): As discussed in Section IV.B, S_1 assumes that all the PEVs start charging simultaneously at 8 PM and have a charging time of 2 hours, which leads to a concentrated charging load during 8-10 PM. Also, as per Section IV.A, SOC^i is assumed to be 20%. These assumptions represent the worst case scenario for the feeder, since full battery charging takes place early, quickly, and simultaneously, coinciding with the system base

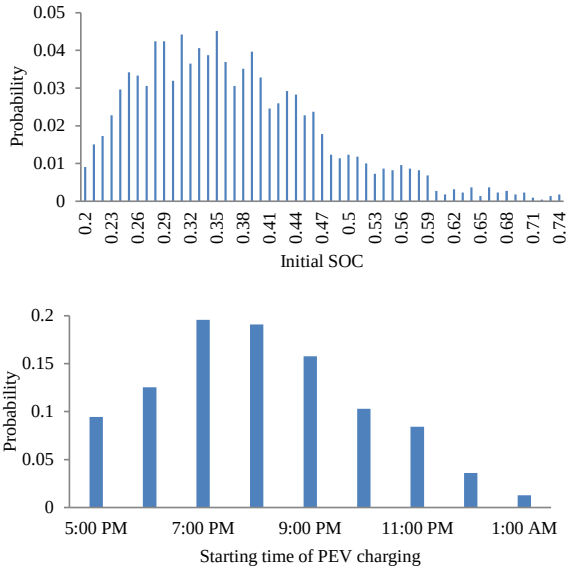

Fig. 18. Lognormally distributed customers' travel pattern for Node 634.

TABLE VIII
PROBABILISTIC STUDIES FOR UNCONTROLLED CHARGING SCENARIO S_1

Expected energy drawn by LDC [kWh]	71,356
Expected feeder losses [kWh]	2,022
Expected PEV charging cost of customers [$/day]	174
Expected cost of energy drawn by LDC [$/day]	3,047

peak demand. However, in practice, the starting time of PEV charging and SOC^i depend on the customers' driving pattern, i.e., miles traveled by the PEV. To model these uncertainties, the starting time of charging and SOC^i are now modeled as lognormally distributed random distributions, as suggested in [30] and shown in Fig. 18, for each load node separately. The above distributions are chosen such that the mean values of the starting charging time and SOC^i are 8 PM and 0.35, respectively, since these can be reasonably considered to be the most likely plug-in time and battery levels for residential customers.

The resulting plots of the probability distributions of the energy drawn by the LDC and the cost of PEV charging obtained from the model are shown in Fig. 19. The expected values of various decision variables are given in Table VIII, noting that these are somewhat lower than those obtained in the deterministic case presented in Section V.A.1., as expected. These results were obtained using a Monte Carlo Simulation (MCS) approach [31].

2) Smart Charging Scenarios (S_3-S_6): As discussed in Section IV.B.2, smart charging scenarios assume an initial SOC of 20%, and a charging window from 7 PM to 7 AM within which the optimal schedules are determined. Unlike S_1, in these scenarios, there is no specified fixed starting time for charging. Since SOC^i depends on the miles driven in the PEVs, this can be modeled using a lognormally distributed probability distribution function (Fig. 18) at each individual load node. For this case, Table IX presents the expected values of various decision variables obtained using an MCS approach,

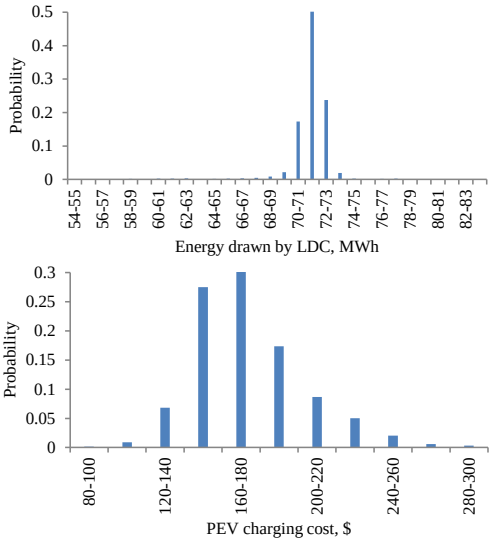

Fig. 19. Decision variable values for probabilistic uncontrolled charging.

TABLE IX
PROBABILISTIC STUDIES FOR SMART CHARGING SCENARIOS

	S_3	S_4	S_5	S_6
Expected energy drawn by LDC [kWh]	67,930	68,029	68,067	72,525
Expected feeder losses [kWh]	1,743	1,710	1,779	2,078
Expected PEV charging cost of customers [$/day]	120	108	90	89
Expected cost of energy drawn by LDC [$/day]	2,853	2,846	2,827	3,016

i.e., energy drawn by LDC, feeder losses, PEV charging cost, and cost of energy drawn by the LDC. The expected values obtained are lower than those obtained in the deterministic case (Table V).

Figure 20 shows four different plots of probability distributions of the decision variables, corresponding to the scenarios in which these variables are being optimized. For example, Fig. 20(a) shows the probability distribution of the energy drawn by the LDC for scenario S_3, which has the objective of minimizing the energy drawn. Similarly, Fig. 20(b) shows the probability distribution of system losses when the LDC's objective is loss minimization (S_4), and so on. These probability distributions depict the range of the values over which the system variables are expected to vary, for the assumed lognormally distributed initial SOCs.

The probabilistic analyses presented here show that the deterministic studies discussed earlier are reasonable, yielding results close to the expected trends for the various relevant variables under study.

E. Real Distribution Feeder

Simulations are also carried out considering a real unbalanced distribution feeder, presented in [32], and depicted in Figure 21. This feeder has three 3-phase transformers equipped with LTCs and a single phase transformer. There are 16 load nodes, with all loads being modeled as constant impedances. The feeder current limit information is not available in this

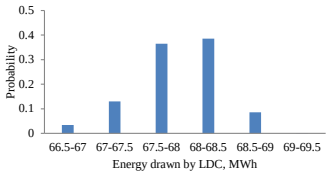

(a) Energy drawn by LDC for S_3.

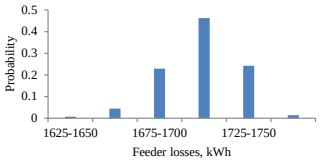

(b) Feeder losses for S_4.

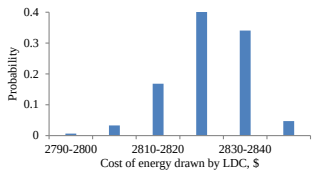

(c) Cost of energy drawn by LDC for S_5

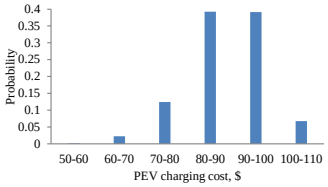

(d) PEV charging cost for S_6

Fig. 20. Decision variable values for probabilistic smart charging scenarios.

TABLE X
NUMBER OF PEVS IN EACH NODE AND PHASE IN THE REAL DISTRIBUTION FEEDER

Node	a	b	c	Node	a	b	c
4	500	502	536	25	-	69	-
6	72	72	72	27	36	-	-
8	250	215	298	30	-	-	46
10	46	46	46	31	41	36	46
13	1	1	1	34	-	-	49
14	50	17	15	36		19	-
22	-	11	-	37	13		11
23	2	-	-	41	170	161	187

case; hence, constraint (20) is not included in the SDPF model. Table X presents the distribution of PEVs at all load nodes and each phase for a 50% PEV penetration.

As described in Section III-A and III-B, uncontrolled PEV charging (S_1 and S_2) and smart charging scenarios (S_3, S_4, S_5 and S_6) are also studied for this feeder. Table XI presents the summary results for the uncontrolled charging scenarios. The improvement in various parameters, such as energy drawn by the LDC, PEV charging costs, etc., in S_2 as compared to S_1 are very similar as for the IEEE 13-node test feeder.

Table XII presents the summary results for the smart charging scenarios. Observe that scenarios S_5 and S_6 result in the same PEV charging cost, since both the LDC and the customers are trying to minimize their respective costs.

It should be mentioned that in the uncontrolled scenario S_2 in Table I, node voltage limits are not considered and thus, the resultant node voltage profiles tend to be lower than the nominal limits. Therefore, since loads are modeled as voltage dependent, they draw less energy from the grid, and consequently incur lower feeder losses as compared to S_3 and S_4, respectively.

It should be noted from the analysis of the results for the two feeders that S_5 is an optimal scenario for both the LDC and the customers. Scenario S_4 results in a fairly uniform load profile, and thus does not require the peak-demand constraint (23) in the SDPF model. Scenarios S_1 and S_6 are extreme scenarios, with S_1 representing the perspective of the LDC only, while S_6 represents the customer interests without concern for the

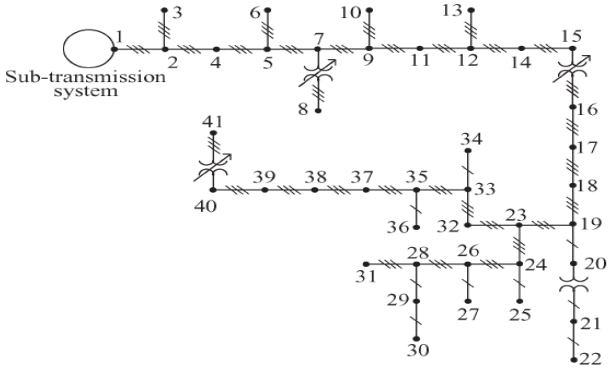

Fig. 21. Real distribution feeder [15].

TABLE XI
SUMMARY RESULTS OF UNCONTROLLED PEV CHARGING SCENARIOS; REAL DISTRIBUTION FEEDER

	S_1	S_2	S_2 vs S_1 change [%]
Energy drawn by LDC [kWh]	276,958	262,858	-5.1
Feeder losses [kWh]	5,045	4,413	-12.5
PEV charging cost of customers [$/day]	867	517	-40.4
Cost of energy drawn by LDC [$/day]	11,580	10,645	-8.1

TABLE XII
SUMMARY RESULTS OF SMART PEV CHARGING SCENARIOS; REAL FEEDER

	S_3	S_4	S_5	S_6
Energy drawn by LDC [kWh]	272,282	275,568	272,397	279,590
Feeder losses [kWh]	4,759	4,612	4,711	5,049
PEV charging cost of customers [$/day]	671	652	617	617
Cost of energy drawn by LDC [$/day]	11,216	11,329	11,165	11,491

TABLE XIII
TEST FEEDERS' STATISTICS

	IEEE 13-node test feeder		Real distribution feeder
	Z loads	ZIP loads	Z loads
Equations	27,014	31,791	66,279
Variables	25,802	30,615	63,507
Model generation time [s]	0.141	0.156	0.483
Execution time [s]	0.172	1.388	2.527

grid. Therefore, scenario S_1 results in minimum energy drawn by the LDC, but at maximum charging cost for the customers, and vice versa for S_6.

F. Computational Stats

The proposed SDPF model has been programmed and executed in the GAMS environment [20] on a Dell PowerEdge R810 server, Windows 64-bit operating system, with 4 Intel Xeon 1.87 GHz processors and 64 GB of RAM. The proposed SDPF model is an NLP problem which is solved using the SNOPT solver [20]. The model and solver statistics for the IEEE 13-node test feeder and the real distribution feeder are summarized in Table XIII.

VI. Conclusions

This paper presented a smart distribution power flow (SDPF) model which incorporates detailed representation of plug-in electric vehicles (PEVs) within a three-phase unbalanced distribution system. The proposed SDPF model is applied to study the effects on distribution feeders of uncontrolled PEV charging vis-*à*-vis smart charging schedules. These smart charging schedules were obtained from the LDC operator's point of view based on various criteria, and considering system operational constraints, and customer's rational behavior.

Studies on realistic test feeders were carried out considering uncontrolled and controlled (smart) charging. The effect of the LDC imposing a cap on system peak-demand was also studied for the smart charging scenarios. Probabilistic studies, to account for different and uncertain customers' travel patterns, were carried out as well for uncontrolled charging and smart charging scenarios to determine the expected values of the various decision variables. The smart charging mode operation was determined to be effective in scheduling the PEV charging loads at appropriate hours, while meeting feeder constraints for the various objectives being considered.

It was observed from these studies that uncontrolled PEV charging can result in violation of grid constraints such as feeder current limits, bus voltages, and may also result in demand spikes. Therefore, controlled mode charging, through smart charging schedules is demonstrated to be the best approach for PEV charging in the context of smart grids.

References

[1] WISE Report to Ontario's Centres for Excellence, "Toward an Ontario Action Plan for Plug-in Electric Vehicles (PEVs)," May 2010.

[2] D. Tuttle and R. Baldick, "The Evolution of Plug-In Electric Vehicle-Grid Interactions," *IEEE Transactions on Smart Grid*, vol. 3, no. 1, pp. 500 –505, March 2012.

[3] "Minitry of Transportation - Ontario." [Online]. Available: http://www.mto.gov.on.ca/english/dandv/vehicle/electric/electric-vehicles.shtml

[4] E. Ungar and K. Fell, "Plug in, turn on, and load up," *IEEE Power and Energy Magazine*, vol. 8, no. 3, pp. 30 –35, May-June 2010.

[5] CanmetENERGY Report, "Electric Vehicle Technology Road Map for Canada." [Online]. Available: http://canmetenergy.nrcan.gc.ca/sites/canmetenergy.nrcan.gc.ca/files/pdf/fichier/81890/ElectricVehicleTechnologyRoadmap_e.pdf

[6] K. Clement-Nyns, E. Haesen, and J. Driesen, "The impact of charging plug-in hybrid electric vehicles on a residential distribution grid," *IEEE Transactions on Power Systems*, vol. 25, no. 1, pp. 371 –380, Feb. 2010.

[7] S. Deilami, A. Masoum, P. Moses, and M. Masoum, "Real-time coordination of plug-in electric vehicle charging in smart grids to minimize power losses and improve voltage profile," *IEEE Transactions on Smart Grid*, vol. 2, no. 3, pp. 456 –467, Sept. 2011.

[8] E. Sortomme, M. Hindi, S. MacPherson, and S. Venkata, "Coordinated charging of plug-in hybrid electric vehicles to minimize distribution system losses," *IEEE Transactions on Smart Grid*, vol. 2, no. 1, pp. 198 –205, March 2011.

[9] S. Shao, M. Pipattanasomporn, and S. Rahman, "Grid integration of electric vehicles and demand response with customer choice," *IEEE Transactions on Smart Grid*, vol. 3, no. 1, pp. 543 –550, March 2012.

[10] D. Wu, D. Aliprantis, and L. Ying, "Load scheduling and dispatch for aggregators of plug-in electric vehicles," *IEEE Transactions on Smart Grid*, vol. 3, no. 1, pp. 368 –376, March 2012.

[11] D. Steen, L. A. Tuan, O. Carlson, and L. Bertling, "Assessment of electric vehicle charging scenarios based on demographical data," *IEEE Transactions on Smart Grid*, vol. 3, no. 3, pp. 1457 –1468, Sept. 2012.

[12] M. Etezadi-Amoli, K. Choma, and J. Stefani, "Rapid-charge electric-vehicle stations," *IEEE Transactions on Power Delivery*, vol. 25, no. 3, pp. 1883 –1887, July 2010.

[13] G. Li and X.-P. Zhang, "Modeling of plug-in hybrid electric vehicle charging demand in probabilistic power flow calculations," *IEEE Transactions on Smart Grid*, vol. 3, no. 1, pp. 492 –499, March 2012.

[14] K. Qian, C. Zhou, M. Allan, and Y. Yuan, "Modeling of load demand due to ev battery charging in distribution systems," *IEEE Transactions on Power Systems*, vol. 26, no. 2, pp. 802 –810, May 2011.

[15] S. Paudyal, C. Cañizares, and K. Bhattacharya, "Optimal operation of distribution feeders in smart grids," *IEEE Transactions on Industrial Electronics*, vol. 58, no. 10, pp. 4495 –4503, Oct. 2011.

[16] C. Chen, J. Wang, Y. Heo, and S. Kishore, "MPC-Based Appliance Scheduling for Residential Building Energy Management Controller," *Smart Grid, IEEE Transactions on*, vol. 4, no. 3, pp. 1401–1410, 2013.

[17] I. Sharma, C. A. Cañizares, and K. Bhattacharya, "Modeling and impacts of smart charging pevs in residential distribution systems," in *Proc. IEEE Power and Energy Society General Meeting*, July 2012, pp. 1 –8.

[18] W. H. Kersting, *Distribution System Modeling and Analysis*, 2nd ed. CRC Press, 2006.

[19] R. Cespedes, "New method for the analysis of distribution networks," *IEEE Transactions on Power Delievery*, vol. 5, no. 1, pp. 391–396, 1990.

[20] "GAMS Solver Description." [Online]. Available: http://www.gams.com/solvers/solvers.htm

[21] Z. Darabi and M. Ferdowsi, "Aggregated impact of plug-in hybrid electric vehicles on electricity demand profile," *IEEE Transactions on Sustainable Energy*, vol. 2, no. 4, pp. 501–508, 2011.

[22] A. Hajimiragha, C. Cañizares, M. Fowler, and A. Elkamel, "Optimal transition to plug-in hybrid electric vehicles in ontario, canada, considering the electricity-grid limitations," *IEEE Transactions on Industrial Electronics*, vol. 57, no. 2, pp. 690 –701, Feb. 2010.

[23] M. Yilmaz and P. Krein, "Review of battery charger topologies, charging power levels, and infrastructure for plug-in electric and hybrid vehicles," *IEEE Transactions on Power Electronics*, vol. 28, no. 5, pp. 2151–2169, 2013.

[24] C. Roe, A. Meliopoulos, J. Meisel, and T. Overbye, "Power system level impacts of plug-in hybrid electric vehicles using simulation data," in *2008. ENERGY 2008. IEEE Energy 2030 Conference*, Nov. 2008, pp. 1 –6.

[25] "IESO." [Online]. Available: http://www.ieso.ca/imoweb/marketdata/hoep.asp

[26] H. Zareipour, C. Cañizares, and K. Bhattacharya, "The operation of ontario's competitive electricity market: Overview, experiences, and lessons," *Power Systems, IEEE Transactions on*, vol. 22, no. 4, pp. 1782–1793, 2007.

[27] "IESO." [Online]. Available: http://www.ieso.ca/imoweb/siteshared/tou_rates.asp

[28] M. C. Bozchalui, H. Hassen, S. A. Hashmi, C. Cañizares, and K. Bhattacharya, "Optimal operation of residential energy hubs in smart grids," *IEEE Transactions on Smart Grid*, vol. 3, no. 4, pp. 1755–1766, Dec 2012.

[29] W. H. Kersting, "Radial distribution test feeders," in *2001 IEEE Power Engineering Society Winter Meeting*, vol. 2, 2001, pp. 908 –912.

[30] M. Shaaban, Y. Atwa, and E. El-Saadany, "PEVs modeling and impacts mitigation in distribution networks," *IEEE Transactions on Power Systems*, vol. 28, no. 2, pp. 1122–1131, 2013.

[31] S. M. Ross, *Introduction to Probability Models*, 10th ed. Elsevier Publisher, 2010.

[32] "Integration of Storage in Electrical Distribution Systems and its Impact on the Depth of Penetration of DG." [Online]. Available: http://canmetenergy.nrcan.gc.ca/sites/canmetenergy.nrcan.gc.ca/files/files/pubs/2009-174_RP-TEC_411-IMPACT_Graovac_Wang_Iravani_e.pdf

Isha Sharma (S'09) received the Bachelors degree in Electrical and Computer Engineering from the University of Windsor, Windsor, Ontario, Canada in 2009. She is currently working toward the Ph.D. degree in Electrical Engineering at the University of Waterloo, Waterloo, ON, Canada. Her research interests are in distribution system modeling and analysis in the context of Smart Grids.

Claudio Cañizares (S'85 M'91 SM'00 F'07) received the Electrical Engineer Diploma from the Escuela Politécnica Nacional (EPN), Quito, Ecuador, in April 1984, the M.S. and Ph.D. degrees in electrical engineering from the University of Wisconsin-Madison, in 1988 and 1991, respectively. He had held various academic and administrative positions at the E&CE Department of the University of Waterloo, Waterloo, ON, Canada, since 1993, where he is currently a full Professor, the Hydro One Endowed Chair, and the Associate Director of the Waterloo Institute for Sustainable Energy (WISE). His research interests are in modeling, simulation, control, stability, computational and dispatch issues in sustainable power and energy systems in the context of competitive markets and Smart Grids.

Kankar Bhattacharya (M'95 SM'01) received the Ph.D. degree in electrical engineering from the Indian Institute of Technology, New Delhi, India, in 1993. He was in the faculty of Indira Gandhi Institute of Development Research, Mumbai, India, during 1993-1998, and then the Department of Electric Power Engineering, Chalmers University of Technology, Gothenburg, Sweden, during 1998-2002. He joined the E&CE Department of the University of Waterloo, Waterloo, ON, Canada, in 2003 where he is currently a full Professor. His research interests are in power system economics and operational aspects.